

Altitude Measurement in Topographic Mapping Based on Barometric Pressure, Temperature, and Humidity using Neural Network

Jatmiko Endro Suseno* and Agus Setyawan

Department of Physics, Faculty of Science and Mathematics, Diponegoro University, Jl. Prof. Soedarto SH, Tembalang, Semarang, Central Java, Indonesia.

Abstract

The Global Positioning System (GPS) has important information and cuts across various sectors. The position of a particular spot is usually stated in coordinates (2D or 3D) based on a specific coordinate system. Simple methods of altitude measuring have been developed in topographic mapping. This study developed an altitude measurement tool using a BMP180 sensor and DHT22 sensor, with calculation from an artificial neural network (ANN) result, based on the influence of the amount of barometric pressure, temperature, and humidity. Output can be displayed through an LCD and a smartphone application, enabled through Bluetooth. The ANN for obtaining altitude values was trained using temperature, humidity, and barometric pressure inputs from places with known high values. The training was conducted in MATLAB. Afterward, the ANN test program Arduino used normalization, denormalization, activation, weight, and bias components obtained from the selected ANN architecture. The Arduino test program showed high output values similar to those from the ANN test, indicating that the test program result is correct. The test results obtained an average error of 6.36%. The advantage of this tool is that it can perform height calculations quickly and easily. Moreover, the tool can further be developed, as training the ANN in various places with more variations in position, height, weather conditions, or height can yield better results.

Keywords: barometric pressure, temperature, humidity, altitude, BMP180, DHT22, artificial neural network

1. Introduction

Nowadays, the use of the Global Positioning System (GPS) cuts across various sectors, including location tracking [1-3], estimating travel routes [4-6], and environment pollution mapping [7-9]. The combination of the information on position and altitude is useful for geophysics exploration, especially gravity and magnetic method, land mapping [10-12], and architecture design [13-15]. However, its application is still limited. The data are taken from a standardized instrument for the height difference. An example of such an instrument is theodolite [16], but theodolite also has weaknesses: several surveys are required to obtain height data, and its operation is complex [17]. One proposed solution is replacing the theodolite and total station instruments using a barometric sensor, which can theoretically measure the height of certain areas at a level [18].

In a previous study, an altitude-measuring instrument with a barometric sensor was developed for measuring height, but other parameters, such as temperature and humidity, were not determined [19]. The research results featured an altitude rate with a high error margin, especially when the measurement was conducted at noon. Therefore, considering this problem, this study aimed to create an altitude-measuring instrument by adding temperature and humidity parameters from a DHT22 sensor. The instrument also used data from the barometric sensor BMP180 as the input to be processed by a neural network to obtain the altitude value. The process of collecting altitude data from the sensor and neural network can speed up and facilitate the usage of the instrument. In addition, a neural network is beneficial to determine the relationship between the input and output; it can group or value the other inputs based on the previous training processes [20].

This study again aimed to develop an altitude instrument using a BMP180 to identify the altitude from a neural network based on the influence of pressure, temperature, and humidity; moreover, the output can be displayed on the LCD and a smartphone application, enabled through Bluetooth connection. Thus, this instrument can

be used as an alternative to the use of theodolite and water pass, which are less practical.

2. Geographical Coordinate System

The position of a particular spot is usually stated in coordinates (2D or 3D) based on a specific coordinate system. The coordinate system is defined with three specific parameters i.e., the location of the zero point of the coordinate system, the orientation of the coordinate axis, and the scale used in defining the particular spot in the coordinate system [21].

One coordinate system is using latitude and longitude to determine the position on Earth. Latitude is the horizontal line centered on the horizon, A +ve value indicates a direction toward the north pole, and a -ve value indicates a direction toward the south pole (angle 0° – 90°). On the other hand, longitude is the vertical line centered in Greenwich, London, which has a +ve value directed toward Hawaii and a -ve value to the opposite (angle 0° – 180°). There are several satellite systems for determining position, such as GPS, from the USA; Galileo, from the EU; the Global Navigation Satellite System, from Russia; and BeiDou Navigation Satellite System (BDS), from China [22].

The altitude is based on the value of the barometric pressure taken. The barometric pressure, as well as temperature, determines the air density. Gravitation makes the air molecules at lower areas denser than those at higher positions. It affects the temperature and barometric pressure. The barometric pressure will decrease when the area is higher, since at higher areas, there are fewer molecules in the air [23].

3. Research Method

3.1 Instrument Scheme

The scheme of the tool to be used consists of two sensors, namely DHT22 for temperature and BMP180 for air pressure. Then the sensor along with the Ublox Neo6m V2 GPS module for the position, a Bluetooth module for communication on a smartphone, and an LCD display for displaying data are directly installed on the Arduino Uno. The scheme of the 3D position instrument is shown in Fig. 1.

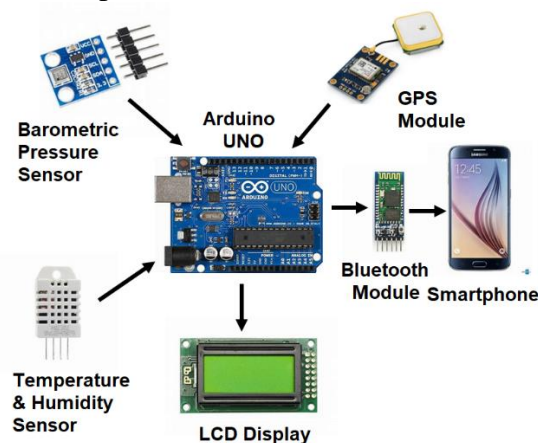


Fig. 1. The scheme of 3D position instrument.

3.2 Instrument Design

The stages of designing an altitude measuring instrument are data acquisition from three inputs: temperature and humidity data using the DHT22 sensor and barometric pressure data using the BMP180 sensor. After installing the reader program on Arduino, data was collected at 10 locations where the standard values for altitude were known. Fig. 2 shows the beam diagrams of the instrument design and the neural network block diagram.

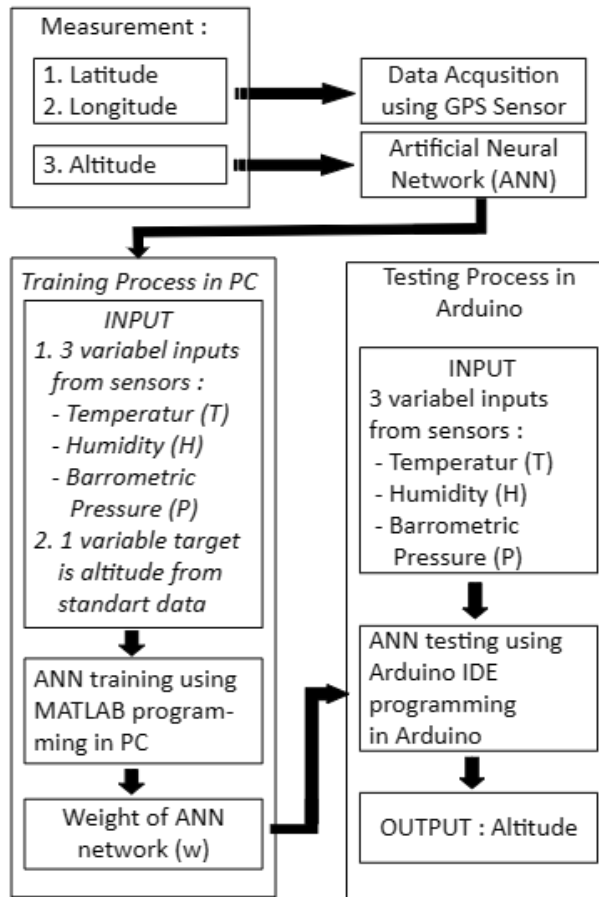


Fig. 2. The beam diagrams of instrument design and neural network block

4. Results and Discussion

4.1 Calibration of DHT22 Sensor

The sensor was calibrated by comparing the temperature and humidity values of the sensor from 8:00 am to 04:00 pm with the standard instrument of those two variables. The temperature sensor calibration showed an average error of 0.26%.

Figure 3 displays the patterns (trends) of the sensor-detected temperature and standard temperature. The data show that both trends are similar. Then, the humidity value from the sensor was also compared with that from the standard device. The calibration of the air humidity sensor showed an average error of 0.98%.

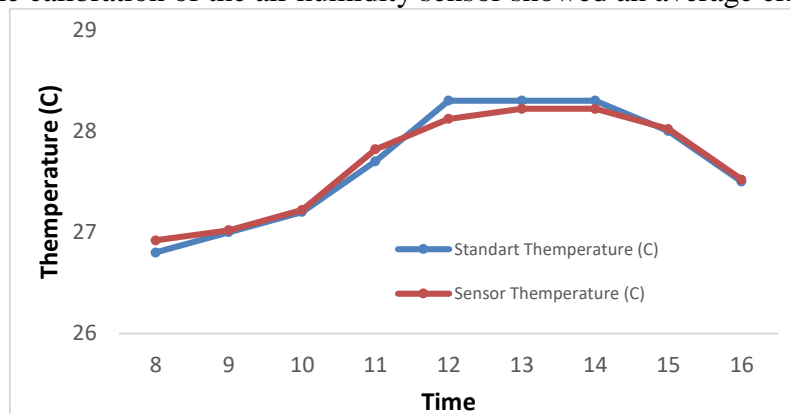


Fig. 3. Graph of sensor temperature vs. standard temperature

Figure 4 displays the trends of the sensor humidity and standard humidity. The data show that both trends are similar. The calibration showed a lowest error of 0.026% and a highest error of 3.77% for the humidity measurement respectively. The difference between the values from the sensor and the standard instrument was caused by the sensor's sensitivity toward its environment; the lower the error the more accurately the sensor measurement.

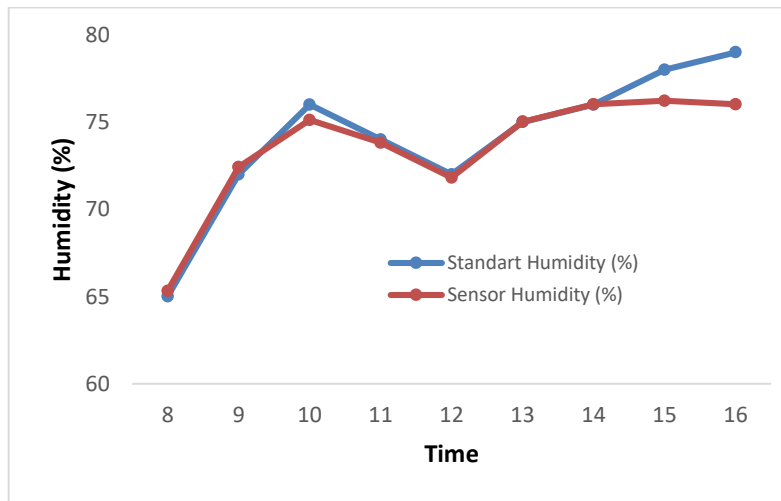


Fig. 4. Graph of sensor vs. standard humidity

4.2 Calibration of BMP180 Sensor

The barometric pressure was calibrated by comparing the sensor value with that of the standard instrument for seven height points. The value of the interval between the points was obtained from the website <https://gps-coordinates.org/distance-between-coordinates.php> by counting the distance of the straight line between two coordinates. The ratio of the barometric pressure value can be seen in Table 3. The calibration showed an average error of 0.051%.

Table 3. Calibration of a barometric sensor

Time	Latitude	Longitude	Barometric Pressure (hPa)		Error(%)
			Standard	Sensor	
16.31	7°2.7480'	110°25.2640'	977.5	978.33	0.08491
16.42	7°2.3820'	110°25.1290'	983.5	984.18	0.06914
16.51	7°2.1830'	110°25.0310'	986.5	986.34	0.01622
16.57	7°2.0820'	110°25.0350'	988.0	988.26	0.02632
17.03	7°1.4950'	110°25.1590'	993.0	992.43	0.05740
17.11	7°0.8120'	110°25.8870'	997.5	997.15	0.03509
17.15	7°0.7110'	110°25.9060'	1000.0	999.29	0.07100
Average error (%)					0.05144

Fig. 5 displays the sensor barometric pressure and standard pressure change trends. The data show that both trends are similar. The calibration experiment showed the lowest error of 0.016% and the highest error of 0.071% for the barometric pressure measurement.

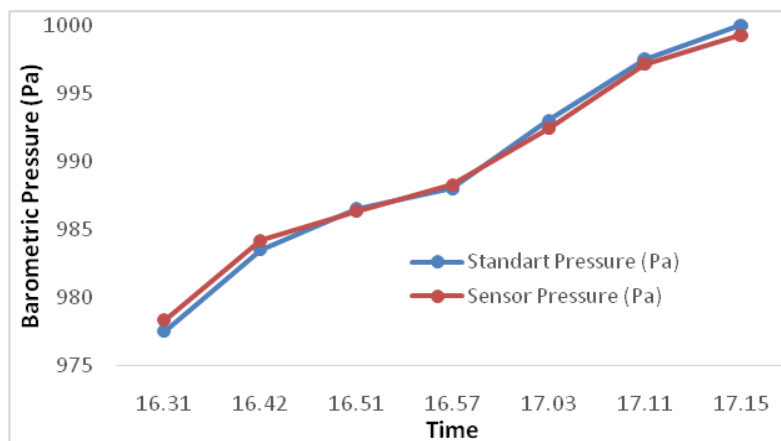


Fig. 5. Diagram of barometric sensor vs. standard

4.3 Result of Neural Network MATLAB Training

The sensor data was used to train the artificial neural network (ANN) in MATLAB. The network used had 1

hidden layer with 20 neurons; the transfer function “tansig” was used for the hidden layer and “purelin” for the output layer. A backpropagation network was used, with the Levenberg–Marquardt (trainlm) training method; the epoch (maximum iteration) was set to 1000, and the goalb (error tolerance) was set to 0. Table 4 presents the comparison of neural network architecture. The lowest error component and epoch were considered in the architecture selection.

Table 4. Comparison of network architecture

No.	Architecture	Error	Epoch	Number of Hidden	Neurons
1	3-2-1	06901	9	2	2
2	3-10-1	09101	6	10	10
3	3-20-1	07086	5	20	20
4	3-25-1	53723	5	25	25
5	3-40-1	46273	6	40	40

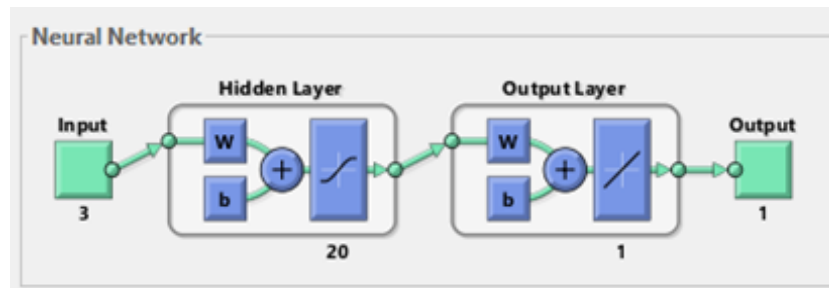


Fig. 6. Neural network architecture

Table 5. Results of network training with MATLAB

No	Code	Time	Altitude(m)	Error (%)	
			Standard Sensor		
1	BM GD03	6.09	190.763	193.01091	0.178373
2	BM GD08	6.12	188.594	188.486	0.057266
3	BM GD04	6.15	184.466	185.9706	0.815652
4	BM GD33	6.18	185.666	185.586	0.043088
5	BM GD34	6.21	186.926	186.9128	0.007062
6	BM GD12	6.24	187.4163	187.3575	0.031374
7	BM GD18	6.28	193.2138	193.2711	0.029656
8	BM GD06	6.30	197.666	197.4916	0.088230
9	BM GD17	6.32	201.544	201.4452	0.049022
10	BM GD15	6.36	203.723	203.3148	0.200370
11	BM GD01	6.38	201.704	201.6855	0.009172
12	BM GD14	6.41	197.968	197.8426	0.063344
13	BM GD20	6.44	203.374	201.5656	0.889199
14	BM GD13	6.47	209.088	208.7054	0.182985
15	BM GD28	6.50	207.5959	207.3946	0.096967
16	BM GD05	6.52	210.096	209.8809	0.102382
17	BM GD11	6.55	210.852	209.2186	0.774667
18	BM GD16	6.58	211.429	210.7893	0.302560
19	BM GD27	7.01	197.7037	197.7611	0.029033
20	BM GD30	7.05	201.726	201.5702	0.077233
21	BM GD31	7.08	202.143	202.9772	0.412678
22	BM GD32	7.10	206.786	208.0738	0.622769
23	BM GD37	7.16	196.1494	196.5884	0.223809
24	BM GD36	7.19	193.457	193.9539	0.256853

25 BM GD35 7.22 187.459 187.9824 0.279208
Average error (%) 0.272918

4.4 Neural Network Testing

After the neural network training in MATLAB, the weight and bias components were used in the neural network testing program Arduino. The Neural Network components to be set are normalization and denormalization as well as activation function. The training data were in the form of temperature, humidity, and pressure. If the result of the research was similar to that of the program, then it was placed in a 3D position to collect the field data.

The data were first collected on February 23, 2020. The test result is presented in Table 6 The results of the network test with MATLAB had the lowest error of 0.46%, the highest error of 4.59%, and an average error of 2.26%. The second data collection occurred on April 3, 2020. The complete input data are presented in Appendix. The results can be seen in Table 7. The results of the instrument field test had the lowest error of 0.58%, the highest error of 16.3%, and an average error of 6.36%.

Table 6. Results of network test with MATLAB

No.	Code	Time	Altitude(m)		Error (%)
			Standard	Sensor	
1	BM GD21	7.18.03	205.8657	201.85	1.950641
2	BM GD22	7.22.49	210.405	203.32	3.367315
3	BM GD23	7.28.05	195.2652	204.23	4.591089
4	BM GD29	7.34.47	205.92885	203.96	0.956083
5	BM D3-FH	7.59.07	204.2857	205.23	0.462245
Average error (%)					2.265475

Table 7. Results of instrument tests in the field

No.	Code	Time	Altitude(m)		Error (%)
			Standard	Sensor	
1	BM GD32	8.30.40	204.69	206.786	1.013608
2	BM GD30	8.33.56	200.54	201.726	0.587926
3	BM GD29	8.37.02	204.55	205.8657	0.639106
4	BM GD27	8.40.29	205.79	197.7037	4.090111
5	BM GD14	8.45.04	201.22	197.968	1.642690
6	BM GD15	8.48.12	210.43	203.723	3.292215
7	BM GD12	8.51.17	216.23	187.4163	15.37417
8	BM GD33	8.53.35	215.87	185.666	16.26792
9	BM GD08	8.56.18	215.66	188.594	14.35146
Average error (%)					6.362135

The highest error from Table 7 is 16.27%; this shows the influence of different conditions of the location on the height determination using ANN with inputs of temperature, humidity, and barometric pressure. From the test conducted in several locations, the following can be summarized:

- Temperature and humidity significantly influence the height measurement, as reflected by the vast difference in the location.
- Temperature and humidity in open areas (which receive direct sunlight or are windy during the data collection) with shady regions or buildings of similar heights can cause vast differences in height measurement by a neural network with temperature, humidity, and barometric pressure inputs.
- The network training is better conducted using data from locations with vast height differences.

4.5 The Instrument Performance and Application Neural Network Testing

The instrument performance and application were good that become with an average error is 6.36% and the result can be acceptable with less than 10%. The results of data read from Arduino Uno can be seen with an

LCD or Android application. Figure 7 shows the initial display of the application. Figure 8 shows the display when the sensor is read directly (live). Figure 9 shows the display when the reading sensor button is pressed. Figure 10 (a) shows the display with the table CSV file, and Figure 10 (b) shows the instrument and LCD.



Fig 7. Initial display



Fig. 8. Display in direct reading



Fig. 9. Display showing sensor data.

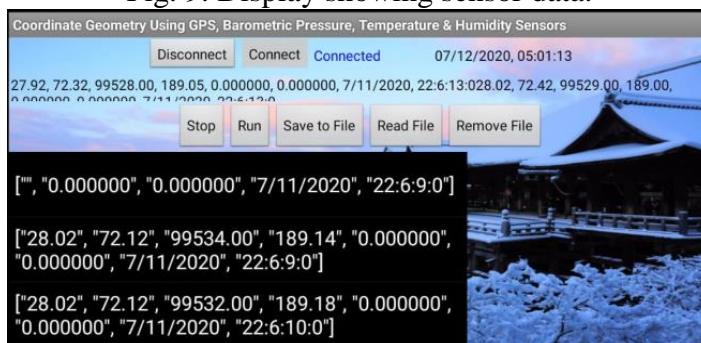


Fig. 10. The instrument

5. Conclusions

In this study, altitude-measuring instruments were developed. The input data are temperature, humidity, and barometric pressure and the output data is altitude. The average error of height obtained from the neural network test data collected is 6.36%. The average error for neural network training was 0.27%. From these data, it can be concluded that in the use of ANN, the environmental conditions where the input data will be taken must be

considered to determine the cause of the existing errors.

References

1. Bajaj, R., Ranaweera, S.L. & Agrawal, D.P., GPS: location-tracking technology, *Computer, IEEE*, , 35(4) pp, 92–94, 2002.
2. Yahya, S.H., Khraisat, Mohammad, A. Z., Al-Khateeb, Yahya K., Abu-Alreesh, Anas, A., Ayyash, Osama, S., & Lahlouh, GPS Navigation and Tracking Device, *i-JIM*, 5(4) pp. 39-41, 2011.
3. Dhanya, N.M., Anti-Theft Vehicle Tracking System Using GPS and Location Prediction, *International Journal on Advanced Science, Engineering and Information Technology*, 8(6)pp. 2584-2589, 2018,
4. Dijk, J.V. & Jong, T.D., Post-processing GPS-tracks in reconstructing travelled routes in a GIS-environment: network subset selection and attribute adjustment, *Journal Annals of GIS*, 23(3), pp. 203-217, 2017.
5. Hardy, A., Hyslop, S., Booth, K., Robards, B., Aryal, J., Gretzel, U., & Eccleston, R., Tracking tourists' travel with smartphone-based GPS technology: a methodological discussion. *Information Technology & Tourism*, 17, pp. 255–274, 2017.
6. Beeco, J.A., & Hallo, J.C., GPS tracking of visitor use: factors influencing visitor spatial behavior on a complex trail system. *J Park Recreat Admin*, 32(2), pp. 43–61, 2014.
7. Beekhuizen, J., Kromhout, H., Huss, A. & Vermeulen, R., Performance of GPS-devices for environmental exposure assessment, *Journal of Exposure Science & Environmental Epidemiology*, 23, pp. 498–505, 2013.
8. Schreiner, C., Branzila, M., Trandabat, A. & Ciobanu, R.C., Air Quality and Pollution Mapping System, Using Remote Measurements and GPS Technology, *Global NEST Journal*, 8(3), pp 315-323, 2006.
9. Adedeji, O.H., Oluwafunmilayo, O. & Oluwaseun, T.A.O., Mapping of Traffic-Related Air Pollution Using GIS Techniques in Ijebu-Ode, Nigeria, *IJG*, 48(1), pp. 73 – 83, 2016.
10. Ismaeel, A.G., New technique for proposing network's topology using GPS and GIS, *International Journal of Distributed and Parallel Systems (IJDPS)*, 3(2), pp. 53–65, 2012.
11. Al-Kadi, I., GPS Satellite Surveying in Developing Countries - A Review, *Journal of King Saud University - Engineering Sciences*, 1(2) pp. 95-109, 1989.
12. L. & Soufi, H., Accuracy assessment of GPS and surveying technique in forest road mapping, *Annals of Forest Research*, 55(2), pp. 309-317, 2012.
13. Xu, R., , Chen, W., Xu, Y., & Ji, S., A new indoor positioning system architecture using GPS signals, *Sensors* 2015, 15, pp. 10074–10087, 2015.
14. Wentao, J., Junming, L, Lina, Y., Yang, Y.X., Xiaopei , Z., Jing, L.V., Qingli, Z. & Maohua, W., Design and implementation of a GPS-based field survey system for land consolidation and rehabilitation projects, *New Zealand Journal of Agricultural Research*, 50(5), pp. 879-885, 2010.
15. Park, H.S., Shon, H.G., Kim, I.S., Park, J.H., Monitoring of Structural Behavior of High-rise Buildings using GPS, *Proceeding of CTBUH 2004 Seoul Conference*, 2004.
16. Usery, E.L., Varanka, D. & Davis, L.R., Topographic mapping evolution: From field and photographically collected data to gis production and linked open data, *Cartographic Journal*, 55(4), pp. 378–390, 2018.
17. Gazi, H.B.A.Ş., The accuracy of using theodolite in close-range engineering measurements, *International Archives of Photogrammetry and Remote Sensing*. Vol. XXXIII, Part B5. Amsterdam, 2000.
18. West, J.B., Prediction of barometric pressures at high altitudes with the use of model atmospheres, 1996.
19. Suseno, J.E., Sitompul, A., Setyawan, A., Gunadi, I., Priyono, Widodo, C.E., Instrumentation of 3D Positions for Topology Mapping Using Global Positioning System (GPS) and Barometric Pressure Sensors, *Advanced Science Letters*, 24(12), pp. 9683–9686, 2018.
20. Cook, N.D., Correlations Between Input and Output Units in Neural Networks, *Cognitive Science* 19, 563-574, 1995.
21. Survey, O., A guide to coordinate systems in Great Britain, Ordnance Survey Adanac Drive Southampton United Kingdom, 2015.
22. Janssen, V, Understanding Coordinate Reference Systems, Datums and Transformations, *International Journal of Geoinformatics*, 5(4), 2009.
23. Brombacher, W.G., Altitude by measurement of barometric pressure and temperature, *Journal of the*

Washington Academy of Sciences, 34(9), 1994.

24. Setiyono, B., Sumardi, & Harisuryo, R., Measurement system of temperature, humidity and barometric pressure over 433 MHz radio frequency: An application on quadrotor, 2015 2nd International Conference on Information Technology, Computer, and Electrical Engineering (ICITACEE). Semarang Indonesia, 2015
25. Pepin, N., Deng, H., Zhang, H., Zhang, F., Kang, S. & Yao, T., An examination of temperature trends at high elevations across the Tibetan Plateau: The use of MODIS LST to understand patterns of elevation-dependent warming, *Journal of Geophysical Research: Atmospheres*, 124(11), pp. 5738–5756, 2019.
26. Lawrence, M.G., The relationship between relative humidity and the dewpoint temperature in moist air: A simple conversion and applications, *Bull. Amer. Meteor. Soc.*, 86 (2), pp. 225–234, 20